ELSEVIER

Journal of Alloys and Compounds 408–412 (2006) 1396–1399

Journal of ALLOYS AND COMPOUNDS

www.elsevier.com/locate/jallcom

Frequency dispersion of complex permeability and permittivity on iron-based nanocomposites derived from rare earth-iron intermetallic compounds

Jiu Rong Liu, Masahiro Itoh, Ken-ichi Machida *

Center for Advanced Science and Innovation, Osaka University, 2-1 Yamadaoka, Suita, Osaka 565-0871, Japan

Available online 23 May 2005

Abstract

Complex permittivity, permeability, and electromagnetic wave absorption properties of resin compacts containing 80 wt% composite powders of α-Fe/Y_2O_3 and ε-Fe_3N/Y_2O_3 were characterized by a conventional reflection/transmission technique. The real and imaginary parts (ε_r' and ε_r'') of relative permittivity for these resin compacts almost kept low constant between 0.5 and 10 GHz. The imaginary part (μ_r'') of relative permeability exhibited a peak in the 1–5 GHz range on the α-Fe/Y_2O_3 resin composites, while "twin peak" dispersion in the 0.5–5 GHz range on the ε-Fe_3N/Y_2O_3 ones. The resin composites of α-Fe/Y_2O_3 and ε-Fe_3N/Y_2O_3 powders with thicknesses of 3.0–5.0 and 3.3–19.3 mm provided good electromagnetic wave absorption performances (reflection loss <−20 dB) in ranges of 2.0–3.5 and 0.6–4.4 GHz, respectively.

Keywords: Melt-spun; Nanocomposites; Electromagnetic wave absorption; Magnetic anisotropy; Matching frequency

1. Introduction

Recent employment of communication devices using the electromagnetic (EM) wave range of 1–5 GHz (e.g., mobile telephones, intelligent transport systems, electronic toll collection systems, and local area network systems) has rapidly expanded. Therefore, the electromagnetic wave absorbing materials have been attracting much attention as anti-electromagnetic interference coatings, and self-concealing technology. For the magnetic EM wave absorbing materials, the complex permeability ($\mu' - j\mu''$), and permittivity ($\varepsilon' - j\varepsilon''$) of materials determine the reflection and attenuation characteristics of absorbers. In addition, since metallic magnetic materials have large saturation magnetization [1,2], and the Snoek's limit is at the higher frequency range, their complex permeability values remain still high in such high frequency range [3]. However, a serious problem is raised when metallic magnetic materials are used as absorbers. The electric conductivity of these materials is generally high, so that the high frequency permeability decreases due to the eddy current loss induced by EM waves. For this reason, it is suitable to use the smaller particles, which are isolated by insulating materials such as epoxy resin. It is well-known that melt-spun technique is an excellent way to produce homogenously microstructured materials with attractive properties for a variety of applications [4–6]. Many workers have investigated that fine α-Fe microstructure can be produced from R–Fe compounds by a hydrogenation–disproportionation reaction. For example, Sm_2Fe_{17} heated over 783 K in a H_2 atmosphere disproportionates into α-Fe and SmH_2 phases [7]. Sugimoto et al. [8,9] have reported good electromagnetic wave absorption properties of the α-Fe/SmO composite derived from the disproportionation reaction of the Sm_2Fe_{17} ingots prepared by arc-melting technique. In this study, the nanocomposite materials of α-Fe/Y_2O_3 were prepared by melt-spun technique, and the electromagnetic wave absorption properties were characterized in the 0.05–20.05 GHz range. In addition, the effect of ε-Fe_3N/Y_2O_3 nanocomposite materials on the electromagnetic wave absorption properties was also investigated because nanometer-sized ε-Fe_3N has larger anisotropy field than α-Fe [10,11].

* Corresponding author. Tel.: +81 6 6879 4209; fax: +81 6 6879 4209.
E-mail address: machida@casi.osaka-u.ac.jp (K.-i. Machida).

0925-8388/$ – see front matter © 2005 Elsevier B.V. All rights reserved.
doi:10.1016/j.jallcom.2005.04.028

2. Experimental

Intermetallic compound ingots of Y_2Fe_{17} were first prepared from Y and Fe metals (>99.9% in purity) by means of arc-melting in Ar. Alloy ribbons of Y_2Fe_{17} with 1.5 mm in width and about 50 μm in thickness were prepared from the above ingots of Y_2Fe_{17} by the single-roller melt-spun apparatus at a roll surface velocity of 20 m/s. After dry ball-milling in Ar, the obtained Y_2Fe_{17} powders with a particle size distribution of 2–4 μm were heated at 873 K in H_2 for 1 h, and then were heated at 523 K for 2 h in O_2 stream. The ε-Fe_3N/Y_2O_3 composites were prepared by nitriding α-Fe/Y_2O_3 powders in NH_3 stream at 623 K for 7 h. The resultant powders were characterized by X-ray diffraction (XRD), and the microstructures were analyzed by a high resolution scanning electron microscope (HITACHI S-5000) and transmission electron microscope (HITACHI H-800). Oxygen and nitrogen contents of the resultant samples were measured by an oxygen–nitrogen analyzer (Horiba, EMGA-550). Magnetization curves of the powdered samples were recorded by a vibration sample magnetometer (Tamakawa, TM-VSM2014-MHR-Type) in a field up to ± 1.6 MA m^{-1}.

Epoxy resin composites were prepared by homogeneously mixing the composite powders at a ratio of 80 wt% with epoxy resin and pressing into cylindrical shaped disks. These compacts were cured by heating to 453 K for 30 min, and then they were cut into toroidal shaped samples with 7.00 mm outer diameter and 3.04 mm inner diameter. The scattering parameters (S_{11}, S_{21}) of the toroidal shaped samples were measured by a Hewlett-packard 8720B network analyzer. The relative permeability (μ_r) and permittivity (ε_r) values were determined from the scattering parameters as measured in the frequency range of 0.05–20.05 GHz. The reflection loss (RL) curves were calculated from the relative permeability and permittivity at the given frequency and absorber thickness according to the following equations:

$$Z_{in} = Z_0 \left(\frac{\mu_r}{\varepsilon_r}\right)^{1/2} \tanh\left\{ j\left(\frac{2\pi f d}{c}\right)(\mu_r \varepsilon_r)^{1/2}\right\} \quad (1)$$

$$RL = 20 \log \left| \frac{Z_{in} - Z_0}{Z_{in} + Z_0} \right| \quad (2)$$

where f is the frequency of the electromagnetic wave, d the thickness of an absorber, c the velocity of light, Z_0 the impedance of air, and Z_{in} is the input impedance of absorber. The attenuation of electromagnetic wave and reflectance of an absorber at the surface were determined from the frequency dependence of reflection loss.

3. Results and discussion

Fig. 1 shows a set of typical X-ray diffraction patterns measured on the Y_2Fe_{17} powders: (a) as-obtained one, (b) after the hydrogenation–disproportionation at 873 K for 1 h in H_2, (c) after oxidizing the hydrogenated sample at 523 K for 2 h in O_2, and (d) after nitriding the oxidized sample at 623 K for 7 h in NH_3 stream. From Fig. 1(a), it was found that single phase of Y_2Fe_{17} was formed by using melt-spun technique. After the hydrogenation–disproportionation, the Y_2Fe_{17} phase was decomposed and the composite powders of both the α-Fe and YH_2 phases were formed as shown in Fig. 1(b). By oxidizing α-Fe/YH_2 powders at 523 K for 2 h, the composite powders of α-Fe/Y_2O_3 were obtained (see Fig. 1(c)). Any peak of Fe_2O_3 phase was not detected on the XRD patterns. However, the peaks of Fe_2O_3 were only observed above 723 K, suggesting that the α-Fe would be oxidized above this temperature. In addition, the oxidized sample at 523 K for 2 h showed the almost same magnetization value ($\sim 1.9 \times 10^{-4}$ Wb m kg^{-1}) as that of α-Fe/YH_2 nanocomposites. Therefore, a two-phase α-Fe/Y_2O_3 composite powders can be obtained by oxidizing α-Fe/YH_2 at the temperature around 523 K. After the nitrogenation in NH_3 at 623 K for 7 h, the XRD pattern of ε-Fe_3N/Y_2O_3 composites was measured as shown in Fig. 1(d), where not only the peaks of Y_2O_3 and ε-Fe_3N were clearly observed, but also the intensity sequence for the peaks of ε-Fe_3N agreed with the previous result reported by Panda and Gajbhye [12]. Nitrogen contents of the resultant ε-Fe_3N_x/Y_2O_3 composite powders were analyzed to be 6.23 wt%, which was correspondent to the composition of stoichiometric ε-Fe_3N ($x = 1$). Mean grain sizes of the Y_2O_3 and ε-Fe_3N particles were evaluated to be about 10 and 30 nm from the line broadening of the X-ray diffraction peaks using the Scherrer's formula. On the TEM photograph of α-Fe/Y_2O_3 composite powders, the particle size of α-Fe/Y_2O_3 was about 1–3 μm composed of α-Fe (~20 nm) and Y_2O_3 grains, which were embedded among the α-Fe crystallites as insulator as shown in Fig. 2(a). The Y_2O_3 grains are too small to be observed. On the SEM photograph of ε-Fe_3N/Y_2O_3 composite powders, the particles were found to be roughly of spherical shape and in a narrow second-particle size distribution with $d = 0.1$–0.2 μm as shown in Fig. 2(b). But such submicrometer-sized second-particles did not be observed

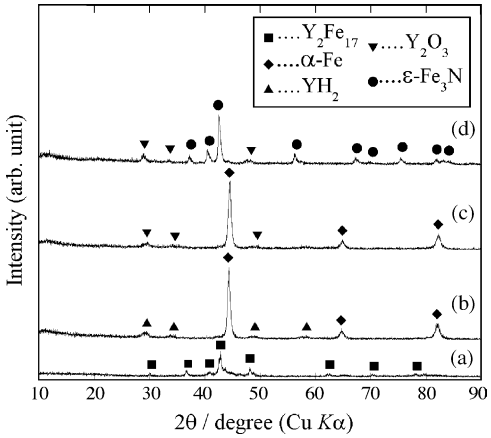

Fig. 1. XRD patterns of the powder samples: (a) as-obtained, (b) after hydrogenation–disproportionation at 873 K for 1 h in H_2, (c) after oxidizing the sample (b) in O_2 at 523 K for 2 h, and (d) after nitriding the sample (c) at 623 K for 7 h in NH_3.

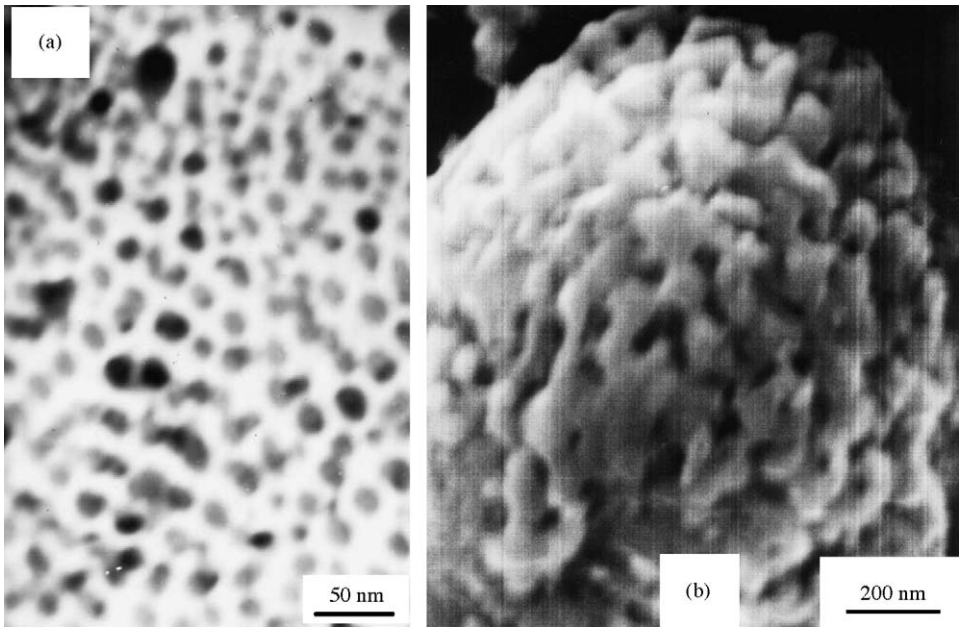

Fig. 2. TEM micrograph of α-Fe/Y_2O_3 powders (a) and SEM image of ε-Fe_3N/Y_2O_3 powders (b).

for the α-Fe/Y_2O_3 powders (see Fig. 2(a)). Therefore, after nitrogenation the particles of α-Fe/Y_2O_3 were decomposed into smaller ones.

Fig. 3 shows the ε_r' and ε_r'' values of relative permittivity for α-Fe/Y_2O_3 resin composites were almost constant between 0.5 and 10 GHz, in which the relative permittivity ($\varepsilon_r = \varepsilon_r' - j\varepsilon_r''$) exhibited less variation ($\varepsilon_r' = \sim 12$, $\varepsilon_r'' = \sim 0.6$). For the ε-$Fe_3N$/$Y_2O_3$ resin composites, the ε_r' and ε_r'' values also kept almost constant ($\varepsilon_r' = \sim 17$, $\varepsilon_r'' = \sim 2.0$) in the 0.5–10 GHz range. The electric resistivity of α-Fe/Y_2O_3 and ε-Fe_3N/Y_2O_3 resin composites was measured to be about 100 Ω m. Such high resistivity is mainly attributed to the epoxy resin embedded among α-Fe/Y_2O_3 and ε-Fe_3N/Y_2O_3 particles as an insulator in the resin composites.

The μ_r' and μ_r'' values of relative permeability are plotted as a function of frequency in Fig. 4. The μ_r' of α-Fe/Y_2O_3 resin composites declined with frequency from 3.4 to 0.76 in the 0.5–10 GHz. However, the μ_r'' first increased from 0.4 to 1.02 with frequency up to 2.7 GHz, and then decreased in the higher frequency range. The μ_r'' curve exhibited a peak in the 1–5 GHz. For the ε-Fe_3N/Y_2O_3 resin composites, the μ_r' declined from 2.45 to 1.04 with increasing fre-

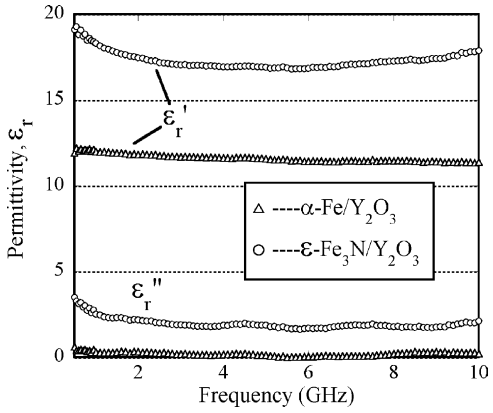

Fig. 3. The relative permittivity plotted against frequency for α-Fe/Y_2O_3 and ε-Fe_3N/Y_2O_3 resin composites with 80 wt% powders.

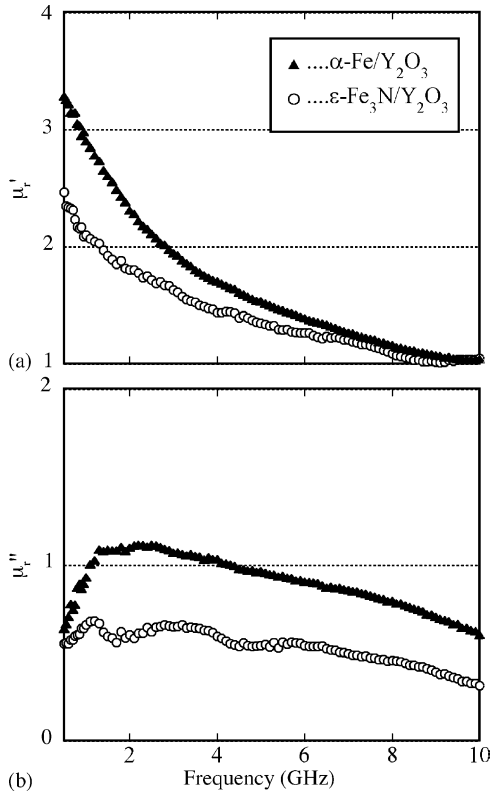

Fig. 4. The μ_r' (a) and μ_r'' (b) curves plotted against frequency for the ε-Fe_3N/Y_2O_3 and α-Fe/Y_2O_3 resin composites with 80 wt% powders.

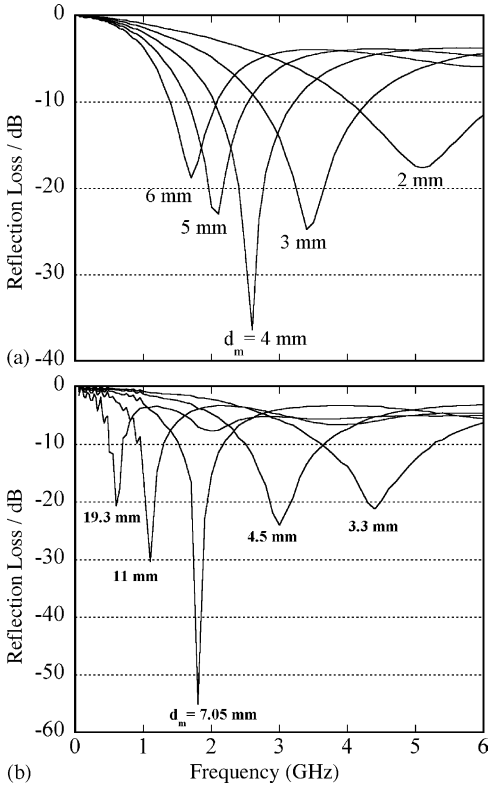

Fig. 5. Frequency dependences of the reflection losses (RL) for the resin composites with 80 wt% α-Fe/Y_2O_3 (a) and ε-Fe_3N/Y_2O_3 (b) powders at different thickness.

quency as shown in Fig. 4. On the other hand, the μ_r'' curve showed "twin peak" dispersion and μ_r'' value retained high in the 0.5–5.0 GHz range, and then decreased gradually in the higher frequency (Fig. 4(b)). This permeability curve can be elucidated as the particle size effect as described by Viau et al. [13] for Fe–Co–Ni elastomeric composites, in which a multiresonant behavior was observed when the size of Fe–Co–Ni particles reduced from micrometer to submicrometer order, e.g. 50–150 nm. Therefore, the μ_r'' curve had two resonance peaks for the ε-Fe_3N/Y_2O_3 resin composites because the second particle size of ε-Fe_3N/Y_2O_3 was 0.1–0.2 μm as shown in Fig. 2(b). Moreover, the ε-Fe_3N/Y_2O_3 composite powders gave the lowered values in both the real (μ_r') and imaginary (μ_r'') parts of relative permeability as shown in Fig. 4. This is due to the fact that the magnetization of ε-Fe_3N is smaller than that of α-Fe.

Fig. 5(a) shows characteristic relationships between the reflection loss and frequency for the resin composite with 80 wt% α-Fe/Y_2O_3 powders. First, the minimum reflection loss was found to move toward the lower frequency region with increasing the composite thickness. Second, the RL value of the resin composite below −20 dB was recorded in the 2–3.5 GHz range. In particular, a minimum RL value of −36 dB was obtained at 2.6 GHz with a matching thickness (d_m) of 4 mm, and the minimum d_m value of 3 mm was observed at 3.5 GHz. For the resin composites with 80 wt% ε-Fe_3N/Y_2O_3 powders, the frequency dependence of RL less than −20 dB was recorded in the 0.6–4.4 GHz range as absorbers with thickness ranging from 3.3 to 19.3 mm, and a minimum RL value of −55 dB was observed at 1.8 GHz with a matching thickness (d_m) of 7.05 mm as shown in Fig. 5(b).

4. Conclusions

The α-Fe/Y_2O_3 and ε-Fe_3N/Y_2O_3 nanocomposites are uniformly prepared by melt-spun technique and the subsequent hydrogenation–disproportionation, oxidation, and nitrogenation treatments. The study of EM wave absorption suggests that the α-Fe/Y_2O_3 and ε-Fe_3N/Y_2O_3 nanocomposite powders can be used as good EM wave absorbing materials in the 2.0–3.5 GHz, and 0.6–4.4 GHz, respectively.

Acknowledgements

This work was supported by Grant-in-Aid for Scientific Research No. 15205025 from the Ministry of Education, Science, Sports, and Culture of Japan, and Industrial Technology Research Grant Program in 2003 from New Energy and Industrial Technology Development Organization (NEDO) of Japan.

References

[1] S. Yoshida, J. Magn. Soc. Jpn. 22 (1998) 1353–1356.
[2] S. Yoshida, M. Sato, E. Sugawara, Y. Shimada, J. Appl. Phys. 85 (1999) 4636–4638.
[3] J.L. Snoek, Physica 14 (1948) 207–217.
[4] H. Kanekiyo, M. Uehara, S. Hirosawa, IEEE Trans. Magn. 29 (1993) 2863–2865.
[5] A. Manaf, R.A. Buckley, H.A. Davis, J. Magn. Magn. Mater. 128 (1993) 302–306.
[6] W.C. Chang, S.H. Wu, B.M. Ma, C.O. Bounds, J. Appl. Phys. 81 (1997) 4453–4455.
[7] M. Okada, K. Saito, H. Nakamura, S. Sugimoto, M. Homma, J. Alloys Compd. 231 (1995) 60–65.
[8] T. Maeda, S. Sugimoto, T. Kagotani, D. Book, M. Homma, H. Ota, Y. Houjou, Mater. Trans. JIM 41 (2000) 1172–1175.
[9] S. Sugimoto, T. Maeda, D. Book, T. Kagotani, K. Inomata, M. Homma, H. Ota, Y. Houjou, R. Sato, J. Alloys Compd. 330 (2002) 301–306.
[10] J.O. Xiao, C.L. Chien, Appl. Phys. Lett. 64 (1994) 384–386.
[11] Z.Q. Yu, J.R. Zhang, Y.W. Du, J. Magn. Magn. Mater. 159 (1996) L8–L10.
[12] R.N. Panda, N.S. Gajbhye, J. Appl. Phys. 81 (1997) 335–339.
[13] G. Viau, F.F. Vincent, F. Fievet, P. Toneguzzo, F. Ravel, O. Acher, J. Appl. Phys. 81 (1997) 2749–2754.